UNIVERSITY OF TARTU
Faculty of Science and Technology
Institute of Technology

Odubena Joseph Theophilus

DETERMINATION OF SURFACE ELASTIC PROPERTIES OF NANOSCALE METAL USING COPPER AND TUNGSTEN AS AN EXAMPLE.

Bachelor's Thesis (12 ECTS)

Curriculum Science and Technology

Supervisor(s):
Prof. Veronika Zadin

Ass. Prof. Andreas Kyritsakis

Tartu 2023

Abstract:

High electric field (HEF) systems such as reactors and colliders operate in extreme environments and are susceptible to breakdown due to two primary reasons: slow-acting structural changes and general material failure. Macro and micro-level studies have shown that HEF systems undergo internal and external structural and mechanical property alterations, leading to damaging occurrences such as vacuum arcs. This phenomenon is characterised by a low burning voltage of approximately 20V and a high current of 35-500A between two metallic electrodes in a vacuum. Anomalies like vacuum arcs can cause significant damage to HEF systems, ultimately leading to general system failure or breakdown, which could have fatal consequences in fields like medicine, biology, renewable energy, and geophysics.

Thus, conducting extensive research and developing theories to explain the failure process and provide possible solutions is crucial. Many scientific studies and theories have highlighted fundamental irregularities in the mechanical properties of materials used in constructing HEF systems, primarily made of 98% Copper as the primary cause. This research aims to contribute to the pool of available data on the surface energy properties of Copper and Tungsten, which is critical data needed to study the HEF system failure phenomena accurately and provide compelling solutions.

Unlike other very complex articles, this thesis provides a step-by-step process for generating accurate data on the surface energy properties of Copper and Tungsten using LAMMPS – a molecular dynamics software, and OVITO – a visualisation tool. While Copper is the primary material used in HEF systems, Tungsten appears to be a suitable alternative due to its material properties, and studying both materials is essential. The data generated will aid in providing a better understanding of HEF system failure and develop more effective solutions.

Keywords:

High electric fields, Molecular dynamics MD, Surface Energy, Surface Elastic Constant, numerical simulations, vacuum breakdown, visualisation tool.

CERCS:

T150 Material technology; T120 Systems engineering, computer technology; Computer technology, numerical analysis, systems, control.

Metalli pinna elastsete omaduste määramine nanoskaalas vase ja volframi näitel.

Lühikokkuvõte:

Kõrge elektrivälja (ingl. lühend HEF) süsteemid, nagu reaktorid ja põrgutid, töötavad äärmuslikes keskkondades ja lagunevad peamiselt kahel põhjusel: aeglaselt toimivad struktuurimuutused ja üldine materjali riknemine. Makro- ja mikrotasandi uuringud on näidanud, et HEF-süsteemides toimuvad sisemised ja välised struktuuriliste ja mehaaniliste omaduste muutused, mis põhjustavad kahjulikke juhtumeid, nagu näiteks vaakumkaarlahendused. Seda nähtust iseloomustab madal, ligikaudu 20V, põlemispinge ja kõrge 35-500A voolutugevus kahe vaakumist ümbritsetud metallelektroodi vahel. Sellised anomaaliad, nagu vaakumkaared, võivad HEF-süsteeme märkimisväärselt kahjustada, põhjustades lõpuks süsteemi üleüldise rikke või purunemise, millel võivad olla saatuslikud tagajärjed sellistes valdkondades nagu meditsiin, bioloogia, taastuvenergia ja geofüüsika.

Seega on ülioluline läbi viia ulatuslikke uuringuid ja arendada teooriaid, et selgitada elektrilise läbilöögi protsessi ja välja pakkuda võimalikke lahendusi. Paljud teaduslikud uuringud ja teooriad on toonud esile HEF-süsteemide ehitamisel kasutatavate materjalide mehaaniliste omaduste fundamentaalsed ebakorrapärasused, mis on peamiselt valmistatud 98% vasest, antud nähtuse peamise põhjusena. Selle uuringu eesmärk on aidata kaasa vase ja volframi pinnaenergia omaduste kohta teada olevate andmete, mis on kriitilised andmed HEF-süsteemi rikete nähtuste täpseks uurimiseks ja veenvate lahenduste pakkumiseks, kogumi kasvatamisele.

Erinevalt teistest väga keerukatest artiklitest pakub see lõputöö välja samm-sammulise protsessi vase ja volframi pinnaenergia omaduste täpsete andmete genereerimiseks, kasutades molekulaardünaamika tarkvara LAMMPS ja visualiseerimisvahendit OVITO. Kuigi vask on põhiline HEF-süsteemides kasutatav materjal, näib volfram oma materjaliomaduste tõttu sobiv alternatiiv olevat ja mõlema materjali uurimine on hädavajalik. Kogutud andmed aitavad paremini mõista HEF-süsteemi tõrkeid ja töötada välja tõhusamaid lahendusi.

Võtmesõnad:

Kõrged elektriväljad, Molekulaardünaamika MD, Pinnaenergia, Pinna elastne konstant, numbrilised simulatsioonid, vaakumi lagunemine, andmete visualiseerimine.

CERCS:

T150 Meterjalitehnoloogia; T120 Süsteemitehnoloogia; arvutitehnoloogia; arvutusmeetodid, süsteemid, juhtimine (automaatjuhtimisteooria).

Acknowledgements

My bachelor's degree program has been an incredible journey in which I have learned much about Science and Technology in General. I am proud to be a member of Vector Lab, where I was trained as a student and accepted as a family in a group of well-experienced doctors and professors in their respective filed. I am excited to see the future work of the group. My gratitude goes out to my thesis supervisor, Prof. Veronica Vahur, for her advice, patience, and guidance throughout this research project. This challenging work would not have been possible without her expertise, especially during my hard times. My thanks go out to Ass. Prof . Andreas Kyritsakis for taking time out of his busy schedule to guide me anytime I have questions. His help and suggestions are greatly appreciated.

Also, gratitude goes out to my deceased parents, Mr and Mrs Odubena, and my siblings, Mrs Bolaji Adedoyin, Mr Kemi Gbao, Mrs Esther Ogunbule, Mr Joshua Odubena, Mr Isaac Odubena, and Pst. Mark Odubena for their love and constant support during my studies at the University of Tartu. Lastly, I would like to thank MFM Scandinavian region for being the reason I am where I am today. Thanks to pastor Mrs Tinuola Olajide for her patience, support, and unconditional love during my graduate studies. These acknowledgements will never be complete if I fail to appreciate my God-sent Father and mentor, papa Weldon Thompson, and his lovely partner Mummy Kathrine. Your love and support for me throughout my undergraduate studies are beyond description; only God can repay you, papa. My love for you both is limitless.

Table of Contents

TERMS, ABBREVIATIONS, AND NOTATIONS

Term (Estonian *termin*)

CERN – Conseil Européen pour la Recherche Nucléaire, or European Council for Nuclear Research

MD – Molecular Dynamics

FEM – Finite Element Method

PFC – Per Fluoro Chemicals

CLIC – Compact Linear Collider

LHC – Large Hadron Collider

EBSD - Electron Backscatter Diffraction

HEF – High Electric Field

Notation (Estonian *mõiste*)

Notations	Meaning	unit
E	Modulus of Elasticity. It could be any of the Modulous such as Young's (**Y**), Bulk (**B**), and Shear (**G**). It is constant in all directions.	Nm^{-2}
σ	Stress induced by the force of deformation.	Nm^{-2}
A	Area of the solid before deformation	m^2
A_0	The new area after deformation	m^2
I	Is the Identity tensor	N
E^{total}	The total energy of a system	Nm^{-2}
$\propto and\ \beta$	Distance between the atom $\propto$ and β	m
γ^{surf}	Surface energy. It is the energy required to create two new surfaces through surface deformation.	Nm^{-2}
A	Area. The area of the simulation box surfaces (Top and Bottom) formed as indicated in Fig 5.	m^{-2}
σ_s	Surface energy standard deviation	Nm^{-2}

INTRODUCTION

The motivation behind this study is aligned with the accelerating demands of energy in the 21st century and the steady rise in global warming. The evolution of greenhouse gases due to the extensive use of fossil fuels for energy production contributes significantly to global environmental warming. Despite the environmental pollution, fossil fuels must be preserved for transportation and other domestic utilities. Alternative means like wind, solar, biomass, and especially nuclear fission energy are under discussion as a significant part of the future energy sources for electricity generation. Besides fission, nuclear fusion technology is also considered an important future energy source due to several advantages over fission technology. However, there are critical issues related to the right choice of materials for smother and longer running of a reactor. The plasma-facing armour material is one of them, and their selection is mainly limited by their heat absorbing and conducting capacity without or with less plasma contamination.

Another motivation for this study is the CLIC Project. One of the highlights of the eighth European Particle Accelerator Conference (EPAC'02), held in Paris on 3-7 June, came from CERN, where the Compact Linear Collider (CLIC) study group has been investigating the use of materials other than Copper for usually conducting accelerating structures. The reason is that LHC, the predecessor of CLIC, which is still doing well, is made up of 98 % copper and therefore suffers material failure from time to time. CLIC is a more significant project. LHC can't simply suffice in the fields needed to produce the high-accelerating gradients the CLIC project aims to achieve. Still, Copper, the material with which the reactor is 98% composed, suffers severe surface damage. The CLIC team believes that this arises from field-emitted electrons that are accelerated from one side of the structure to the other, causing melting and erosion of the coupling irises (regions of smaller radius separating the cells of an accelerating system). A solution to this problem has not yet been found; hence CLIC project is delayed.

This project intends to use the model study of Copper developed in this study to study Tungsten (W) as a potential replacement. This thesis assumes that by replacing Copper with Tungsten, CLIC might withstand high gradients for several thousands of hours without surface damage.

Why might Tungsten (W) be a viable option?

Tungsten is an excellent PFC material candidate and has been chosen for the ITER divertor because of its superior thermomechanical properties, such as its high melting point, mechanical strength, thermal conductivity, and high resistance to chemical erosion and its high energy threshold for physical sputtering. Previous studies have demonstrated that surfaces of solids possess interesting properties because they possess atoms with fewer neighbours and, consequently, excess energy than atoms in the bulk. The properties of surfaces dominate processes ranging from intercellular transport in biological systems to the growth of thin films used in microelectronic devices. An essential property of solid surfaces is surface stress. When a liquid surface is deformed, atoms from the bulk can migrate to the surface so that the number of atoms per unit area remains roughly constant in the deformation process.

Researchers at the Los Alamos National Laboratory in the United States have developed thin films made of a tungsten alloy that could be used inside fusion reactors. The nanocrystalline tungsten-tantalum-vanadium-chromium alloy material showed outstanding radiation resistance compared to pure nanocrystalline tungsten materials. The inside of a fusion reactor vessel faces the hot plasma and must withstand extremely high temperatures and bombardment by charged and neutral particles. Tungsten, currently considered the most suitable material to protect the inside of a vacuum vessel, tends to fracture after radiation, while the newly developed alloy material retains its mechanical properties.

1. LITERATURE REVIEW

1.2 Theories of system breakdown

One frequently observed problem in high electric field systems out of many is system breakdown caused by vacuum arcs. Vacuum arcs is an electrical glitch that happens near metal surfaces due to different processes going on in the surface and subsurface layers of metals in the presence of high electric fields. It is detected by a voltage drop and a high electron current, significant power consumption, and eventual system shutdown.

As earlier stated, these failures are never non-lethal, when the impact of the system it affects (Collider and reactors) in the field of Medicine, Biology, Renewable energy, and Geophysics, to mention but a few are considered to be fatal. Many studies have been conducted in an attempt to explain the mechanism involved in the failures. A study by [1] reveals that for vacuum arc, a leading cause of failure in HEF systems, to occur, there must be the presence of nano protrusion from the metal surface. These protrusions can emit an electric field current strong enough to spark the electric glitch in a high electric environment to initiate the arc. The study reveals that surface irregularities of dimension 100 nm or less must be present to serve as the emitter. Using molecular dynamics simulation, [2] demonstrated how atomic bond breakage is possible in atomic metal structures in high electric fields as a possible explanation for the formation of the nanoparticles for breakdown to occur. In continuation, [3] further studies reveal the field effect of these atomic emissions on the breakdown mechanism.

While theories and studies for a possible explanation for system breakdown are numerous, the studies postulating vacuum arc propelled by the presence of tiny nano protrusion initiating the breakdown stand out. Still, none of the studies above has addressed how the nano protrusion or surface roughness comes to be. However, upon further research, several other studies link fundamental material structure and properties as the primary source. For instance, [4], in his study, showed a significant relationship between material lattice type and its ability to withstand surface cracks and eventual breakdown. Another study by [5] links the formation of nanoparticles and eventual breakdown to the probability of dislocation motion of atoms when stress is induced. Finally, considering all studies on the subject matter, it is clear that it all boils down to understanding the mechanical properties of the material used to build HEF. As a result, [6] reveal how studies of surface properties like surface energy and surface elastic constant of crystalline metal at the atomic or micro level help understand the mechanical properties of these metals and, eventually, the failure phenomenon associated with HEF.

1.3 Understanding structure and terminology of solids (metals)

Understanding the structure and terminology of solid materials is essential to understand in more explicit detail the metal material's entire (surface and bulk) behavioural properties. Without understanding these basic terminologies, it will be nearly impossible to understand how and to what degree the structure (bulk - internal and surface -external) affects the properties and, by extension, the behaviour of the solid material in an extreme environment. It is in this regard that some of the terminologies are highlighted below.

1.3.1. Crystal structure

The term crystal structure in solid mechanics refers to solids, e.g., metals whose arrangement of atoms or molecules are in an orderly repetitive manner with consistency; the word amorphous is the exact opposite. Furthermore, the pattern with which the atom of crystalline solid form is known as a crystal lattice.

1.3.2. Crystal lattice.

A crystal lattice is a crystal structure formed when the group of atoms is arranged identically at the lattice point. The group of atoms or molecules is called a basis. Lattice point is an imaginary concept.

1.3.3. Unit Cell

Unit cells can be considered the building block of a crystal. It has the same symmetry as the entire crystal. As a result, all crystalline solids like Copper and Tungsten can each be grouped into one of the three general categories.

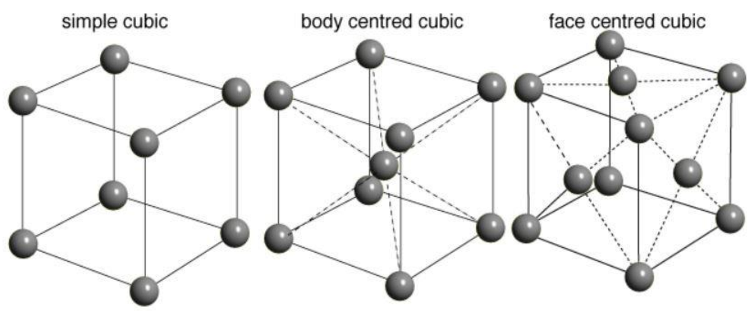

Figure 1. Unit lattice of crystalline solids

Body-centred cubic (BCC) represents the unit cell of BCC crystalline solids. In **bcc crystalline solids,** one atom is directly in contact with eight other atoms or lattice points. Examples of BCC crystal lattice structure metals are vanadium, **Tungsten**, and chromium.

Face-centred cubic (FCC) represents the unit cell of FCC crystalline solids. In **fcc crystalline solids,** one atom is directly in contact with four other atoms or lattice points. Examples of FCC crystal lattice structure metals are **Copper**, lead, and nickel.

1.3.4. Crystallography, crystallographic orientation, and Miller indices.

The study of the atomic structure of crystalline solids is called Crystallography. It is also defined as the experimental and applied study of crystalline structures and how their atoms are arranged. Crystal orientation measurement is a major application of EBSD. To specify lattice planes or crystal surfaces, Miller indices are used.

1.3.5. Miller indices

These are the symbolic vector representations for the orientation of an atomic plane/surface in a crystal lattice and are defined as the reciprocals of the fractional intercepts the plane makes with the crystallographic axes. It is a universal convention for identifying different crystal surfaces a crystal solid might have or can have. Figure 2 below shows a solid material's crystal surface, 3 of which will be our study point for Copper and Tungsten.

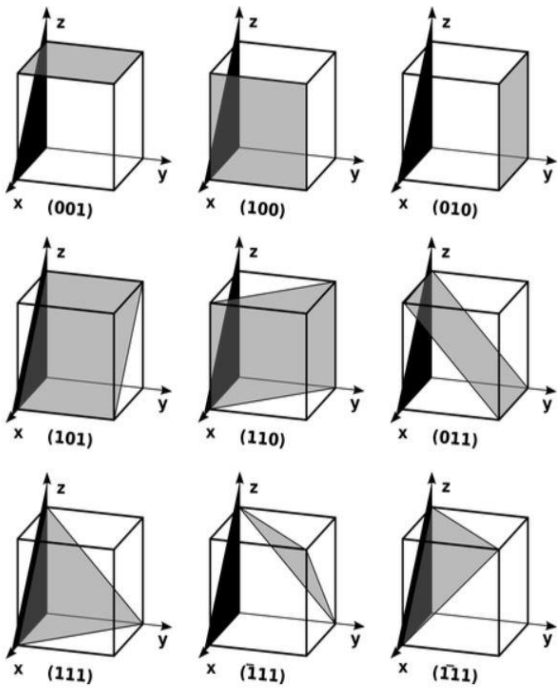

Figure 2. Examples of crystal lattice planes in metals.

In FFC and BCC metals, there are several crystal planes orientation, But for these studies on - Cu and W, we will be concentrating on (001), (110) (111) surfaces.

Choosing a crystalline substrate (of any known metal) with a specific crystal orientation (surface) is a standard procedure in material modification that helps in the production of different materials with specific desired features.

1.4 Common phenomenon of solids Materials (e.g., metal)

1.4.1 Engineering Stress and Strain

When deformation forces act on a material, the effect is felt from the internal structure to the material's surface. A known method for studying the impact of the deformation force or its action on the behavioural properties of the material is through the strain-stress curve. Hence strain-stress curve tells a great deal of important graphical measures of the mechanical properties of solid material. Parameters from the Strain- stress curve analysis provides us with deeper important information on beneficial solid mechanical properties like the Modulus of Elasticity - Young's, Bulk and Shear, and Elastic constant of the material in question. Hence, to test the material's properties before its industrial application, a known artificial stress-strain test known as the Tensile test is performed to obtain the stress-strain curve for analysis.

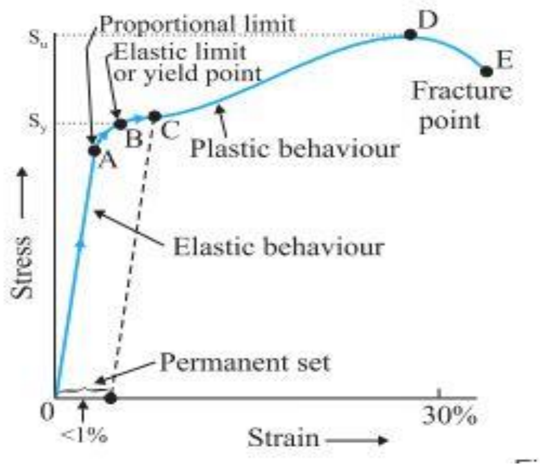

Figure. 3 Typical stress-strain curves of solid under the action of deformation

Fig. 3 is a typical example of a solid undergoing the influence Tensile test via an artificial deformation force. Under the action of this force, stress naturally begins to build up within the material's internal structure. According to Hooke's law: the solid of most materials, under the action of a force of deformation, experience stress, and the accumulated stress result in a resultant strain (the change in parametric length of the material) so much so that for as much as the elastic limit isn't reached the strain produced is proportional to the induced stress.

Mathematically Hooke's Law is interpreted as;

$$\sigma = E * \varepsilon \qquad\qquad eqn\ (1)$$

Where E is Young's modulus (Gpa),

Reading the stress-strain graph at a glance;

Although reading the stress-strain curve beyond the elastic limit point is tricky, many profound predictions can still be made. In Fig 3., the region marked O – A is observed to have linearity because this is the region below the elastic limit/yield point where Hooke's law - stress is proportional to strain is valid. This implies if the force inducing the stress is taken away, the material or surface can still assume its original shape or structure.

Point B in the curve is the Yield Point or the elastic limit, and the corresponding stress is the material's Yield Strength (Sy). Once the load is increased further, the stress starts exceeding the Yield Strength. This means that the strain increases rapidly, even for a slight change in stress.

This is shown in the region from B to D in the curve. The body does not regain its original dimension if the load is removed at a point C between B and D. Hence, even when the stress is zero, the strain is not zero, and the deformation is called plastic deformation.

Furthermore, point D is the material's ultimate tensile strength (Su). Hence, a fracture can occur if an additional strain is produced beyond this point (point E). If The ultimate strength and fracture points are close to each other (points D and E), then the material is brittle. The ultimate strength and fracture points are far apart (points D and E), and the material is ductile.

1.4.2 Dislocation Motion

As established under the tensile test, solid materials undergo elastic deformity. Any further stress beyond the ultimate tensile stress of a particular metal material leads to a defect known as dislocation. Dislocation occurs in a material when a plane of the material slips adjacent to the corresponding plane, leading to a mismatch in the material's atomic structure or configuration.

1.4.3 Theory of Structural Deformation in solid material

Materials in free space are constantly under more than one type of force acting on them, either from above or below them. One example of such forces is the gravitational pull of the earth acting on all things on the planet. These forces could be naturally occurring forces – depending on the environment/field from which the force is generated could also be human-induced forces, as in the Tensile test (stress-strain test) experiment mentioned above. In the case of this thesis, the forces acting on the surface of our material are high electric and magnetic and temperature influenced field generated forces. Regardless, all forces acting on any solid material have one intent, to displace atoms or atomic arrangement via a dislocation motion, i.e., to deform it.

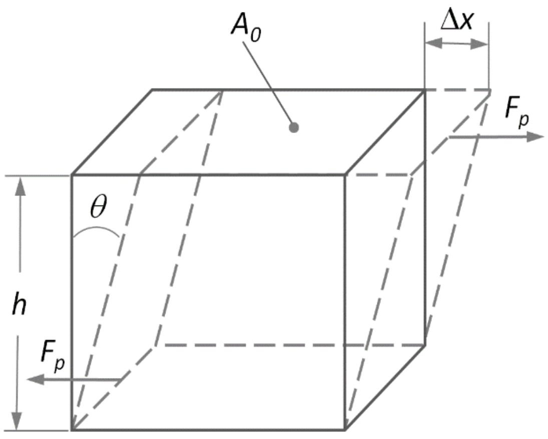

Figure. 4 examples of solid material undergoing forces of deformation

To put it in proper context, Fig. 4 is an example of solid undergoing forces of deformation. Under this force's influence, the solid's internal atomic structure is disfigured, making the solid take a new physical form. These deformation forces lead to external changes in lengths and heights, resulting in a new area A_0. Therefore, the relationship between the surface deformation Force F_p and new area A_0 can be mathematically represented as:

$$A = A_0 \det F \qquad eqn\ (2)$$

And then.

$$A = A_0 \sqrt{\det(\boldsymbol{I} + 2 \in)} \qquad eqn(3)$$

1.5 Properties of solid surface

1.5.1 Why the surface?

As previously established, in material production, the surface (the particular crystallographic plane made to be the exposed or outermost layer of metal) reflects all phenomena and properties of the whole materials as mentioned above but differently. This makes the material's surface properties a crucial study of this work as it lays the foundation of what anomalies occur in HE Systems. As a matter of research, studies have shown that understanding of surface properties of metals is crucial from both scientific and technological viewpoints.

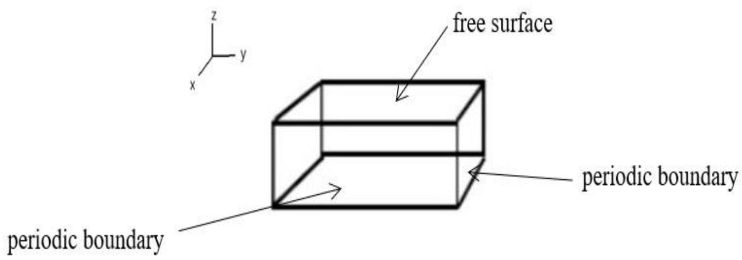

Figure 5. Example of metal surface structure.

As many studies revealed, surfaces of metals, according to crystallographic plane research, have different packs and arrangements of atoms. This pack and structure influence the energy signature of the surface and, eventually, the material property and functionality of the metal in its application process. Nevertheless, according to the principle of continuum mechanics, the study of solid material property involves the study of the bulk + surface as indicated. Since property study is the objective of the thesis, all tests, results and studied properties are done by Lammps simulation software, and the result is visualised using Ovito visualisation software.

2. THE AIMS OF THE THESIS

- To establish a step-by-step guide by means of Molecular Dynamics studies using LAMMPS software and visualisation software on how material properties like surface energy and surface elastic constant are studied.
- Use this model developed from studying and affirming the properties of Copper to an agreeable degree to check the same property for Tungsten (W) which are needed for developing the Finite element model for the breakdown simulation using Tungsten as a replacement for Copper and perhaps be able to come to an established conclusion if Tungsten (W) will be a better material in terms of property for CLIC use case.

3. EXPERIMENTAL SETUP

Table 1. Lammps simulation box details for both Cu and W

	Simulation box	
	Bulk	Surface slab
Box size	25 x 25 x 25 nm	25 x 25 x 25 nm
boundary condi-tions	All three directions, x, y, and z, are periodic	Both x and y directions are periodic, and z is fixed
Temperature	300 K	300 K

Simulation procedure

The simulation and test from this point onward are done to put together a tested and tried lammps script for calculating the Surface energy of three crystal surfaces of mainly Copper and then proceed to use the established script for obtaining the surface energy of Tungsten. Verification of the written script was done using the same script for calculating the surface energy of several other FCC crystals and tested with different EAM potentials before using the same to get the surface energy for Tungsten which is all that is needed for this.

The script was written in a way that the MD simulations were first run at zero kelvin, a necessary step needed to find the lattice constant of the atom of the element being studied. This is then used for setting the simulation box dimension, as indicated in Table 1.

Two simulation boxes were created for each box dimension above to find the surface energy. One slab represents the bulk, and the other represents the surface with an open boundary in the z-direction. In both simulations, energy minimisation was performed such that the atoms at the surface relaxed to their equilibrium positions, a strain rate between 0.003 and 0.01 was applied at the different principal directions and then the potential energy, cohesive energy and other useful parameters from both simulations where obtained for basic calculations to get the surface energy. Dump files were also obtained for Ovito visualisation. It is also worth noting that the simulation was done in steps of 0.001 time steps and 200,000 runs.

3.1. MATERIALS AND METHODS

3.1.1 Lammps

Developed at Sandia National Laboratories USA, LAMMPS (Large-Scale Atomic/Molecular Massively Parallel Simulator) is an open-source code. As a computational software tool, Lammps is widely used for simulation studies of the properties of liquids and solids at the molecular level. MD simulations are done in lammps by script writing. These scripts are lammps commands readable by the software. All scripts used for this thesis are either direct or modified scripts provided by Sandia Labs and publicly available for general use. Lammps scripts are written as a line of special commands in text format, and this script pattern requires a fundamental setup. The setup could be summarised into four parts.

Table 2. Summary into four steps, how lammps script looks like

1. Initialisation	**2. simulation cell/box and atom set**	**3. Force field setting**	**4. Run**
This part entails setting up of • Unit style • Boundary condition • Simulation dimensions, e.g., 2D/3D on which the entire simulation runs.	setting up of simulation box/cell and the atoms to fill them with via commands like • **Region.** • **Create atom.**	This part entails defining the force field with which atom of the metal in question reacts and calling up the file, which provides lammps with the information via commands like. • **Pair_style.** • **Pair_coeff.**	This part entails where • Energy minimisation • Energy Relaxations • And eventual **running** of the entire setup. Is carried out

For lammps to successfully simulate the motion of an atom from time to time and then visualise through the Ovito software, it must be able to predict atomic position in time. This is made possible in lammps software via the equation.

$$E^{total} = \frac{1}{2}\sum_{\propto}\sum_{\beta\neq\propto}\emptyset\left(r_{\propto\beta}\right) + \sum_{\propto}F(\rho_{\propto}) \qquad eqn\ (4)$$

3.1.2 EAM potential

Atomic potentials are computer-generated and readable files of different formats created and stored in the potential interatomic repository of Sandia Lab website for general use by lammp scripts and users. The Potentials force field, as they are called, is the representative of the metal element to be studied. A potential file of Copper is all properties of Copper represented in numerical data format to be used to study various properties of Copper, for example. Hence many potentials are used for different purposes, but arguably the Embedded Atom Method potential (EAM) is widely used and accepted for studying metals and their properties (e.g. Surface energy)

MD simulation is a unique tool used to model atomic behaviours and properties under a determined state; it does that well in combination with the force field file, otherwise known as potential. This equation, in line with my modelled simulation, was used in this thesis to get the surface energy properties of any element from their potential.

$$\gamma^{surf} = \frac{E^{tot} - NW_{bulk}}{2A} \qquad eqn\ (5)$$

3.1.3 Standard Deviation ($\boldsymbol{\sigma}$)

The standard deviation is a measure of the amount of variation or dispersion of a set of surface energy values. A low standard deviation indicates that the values are close to the mean of the surface energies per time. In contrast, a high standard deviation indicates that the surface energy values are spread over a broader range.

$$\sigma_s = \sqrt{\frac{\sum(x_i - \mu)^2}{N}} \qquad eqn\ (6)$$

4. RESULTS and DISCUSSION

This section contains the results of surface energy calculations. Out of several, the surface energy of three important surface orientations was studied, namely: (001), (110) and (111). The first study in Table 2 was conducted to compare with other results by theoretical calculations and experimental measurements. Embedded atom potentials by [7] and [8] were used to perform this study. Figure 7 is the visual result of atomic arrangement on different surfaces of both Copper and Tungsten. The pictures are obtained from Ovito visualisation software. How these atomic arrangements on various surfaces affect the various surface energies is anisotropic and will be examined in detail later, with further results. Besides Ovito visualisation software, graphic results were generated via Octave online software similar to MATLAB.

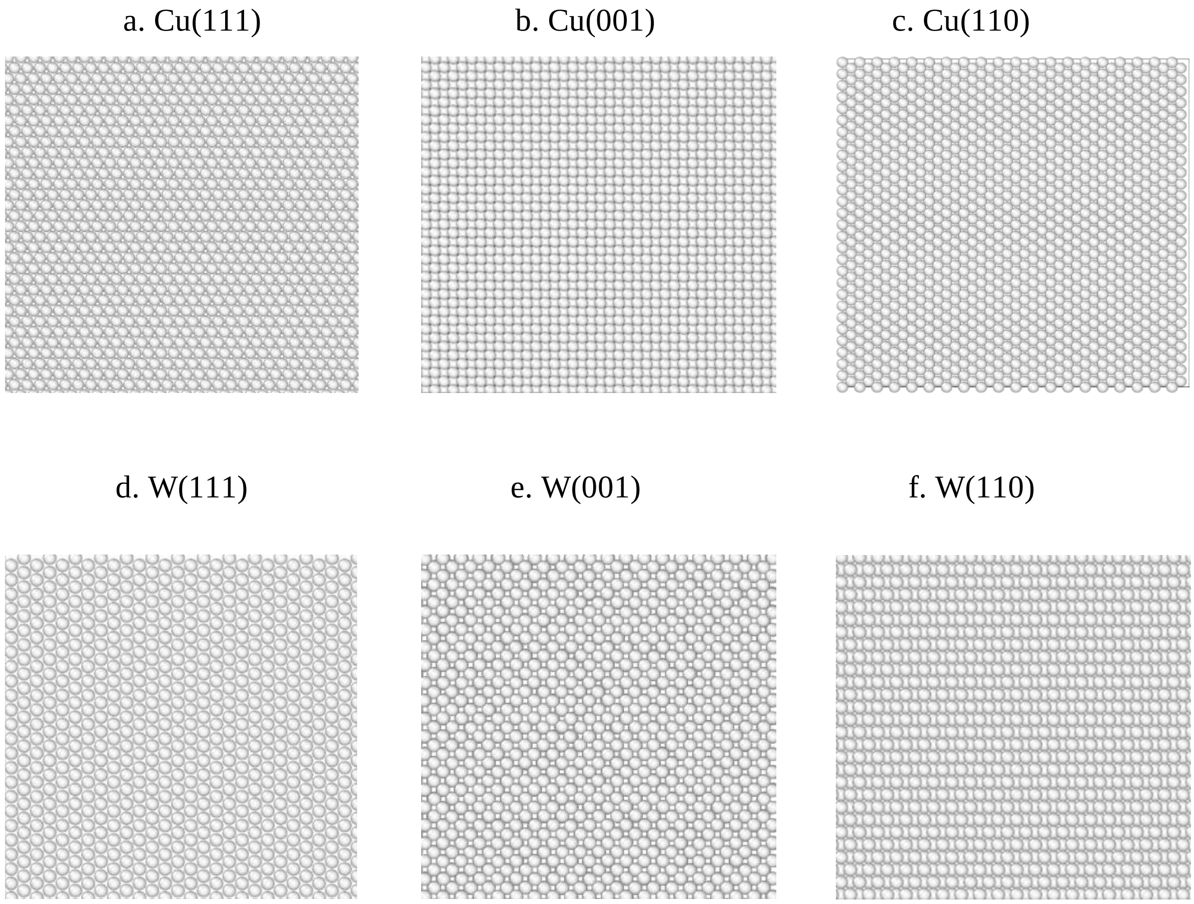

Figure 7. Snapshot of simulated structures.

4.1 Test and results

Figure 8 -16 is the visual result of atomic arrangement in different surfaces of Copper and Tungsten and how this affects the surface energies. The pictures are obtained from Ovito visualisation software, and graph generation is done by Octave online software similar to MATLAB.

Below are the long-term simulation results of Copper and Tungsten surface energy at 400K and different seeds.

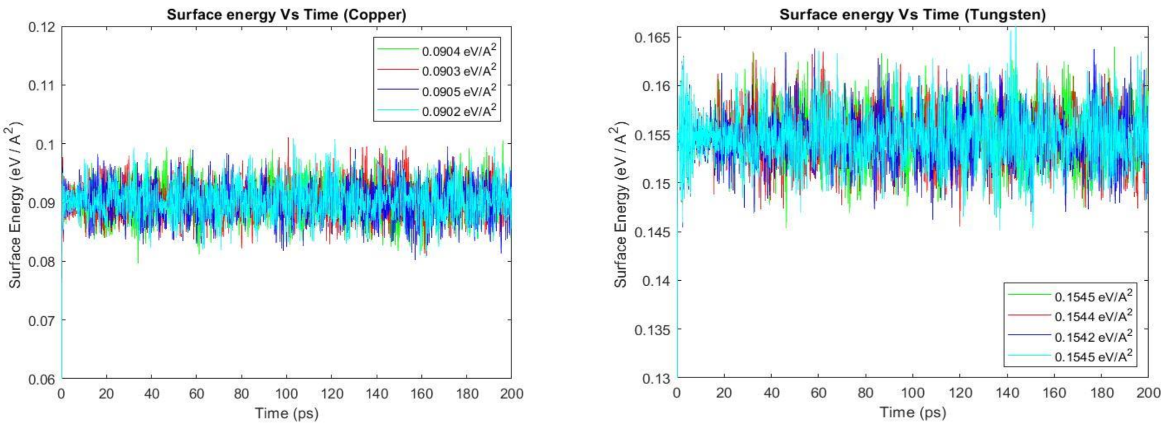

Figure 8. Long-term simulation of the surface energy of Cu and W at 400K and different seeds

Figure 8. above shows the long-term simulation results of Copper and Tungsten to see if and how both systems converge and stabilise. As expected from the results above, we could see some oscillation and no long-term trends, making it good enough for the studies to proceed to data extraction and further study analysis.

Below are the results of the surface energy of Cu and W at 300k and at different seeds.

(a)

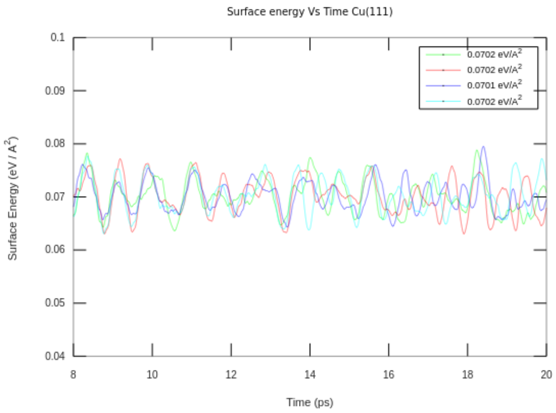

(b)

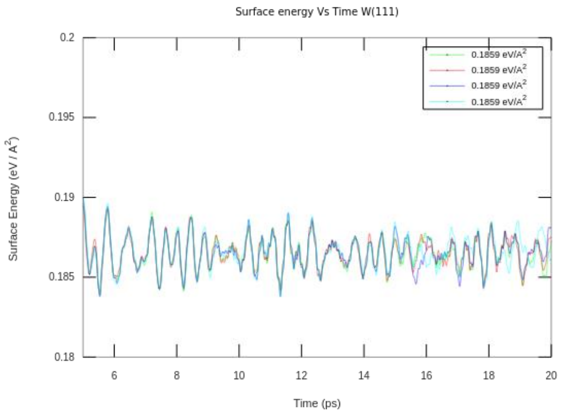

(c)

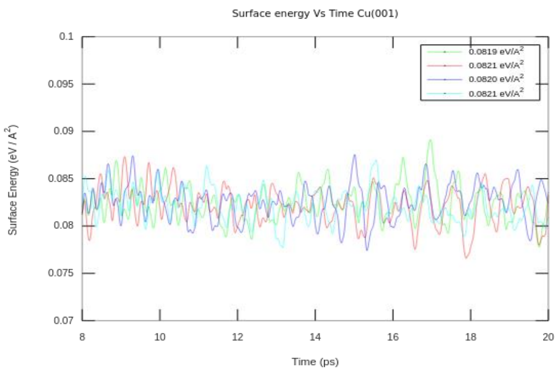

(d)

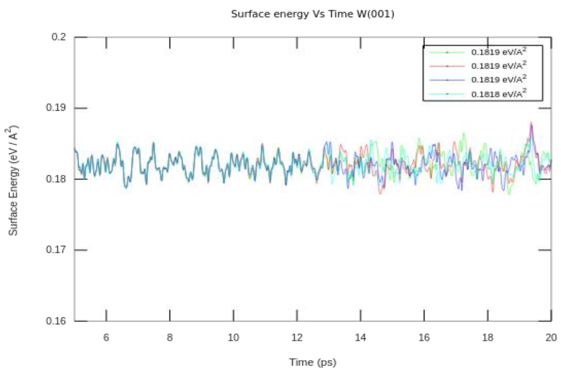

(e)

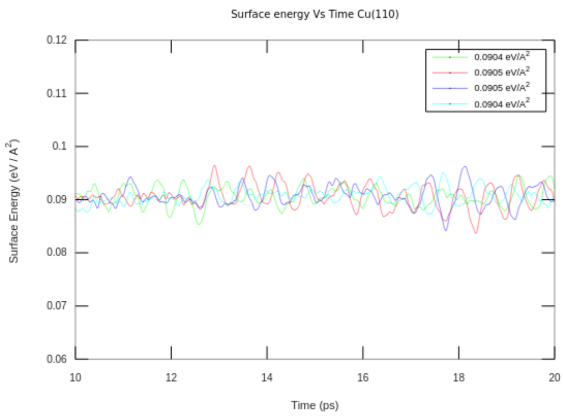

(f)

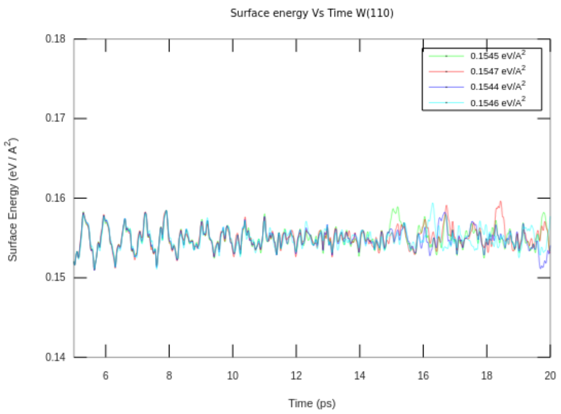

Figure 9. Surface energy of Cu and W at 300K and different seeds

Below are the results of the surface energy of Cu and W at 350k and at different seeds.

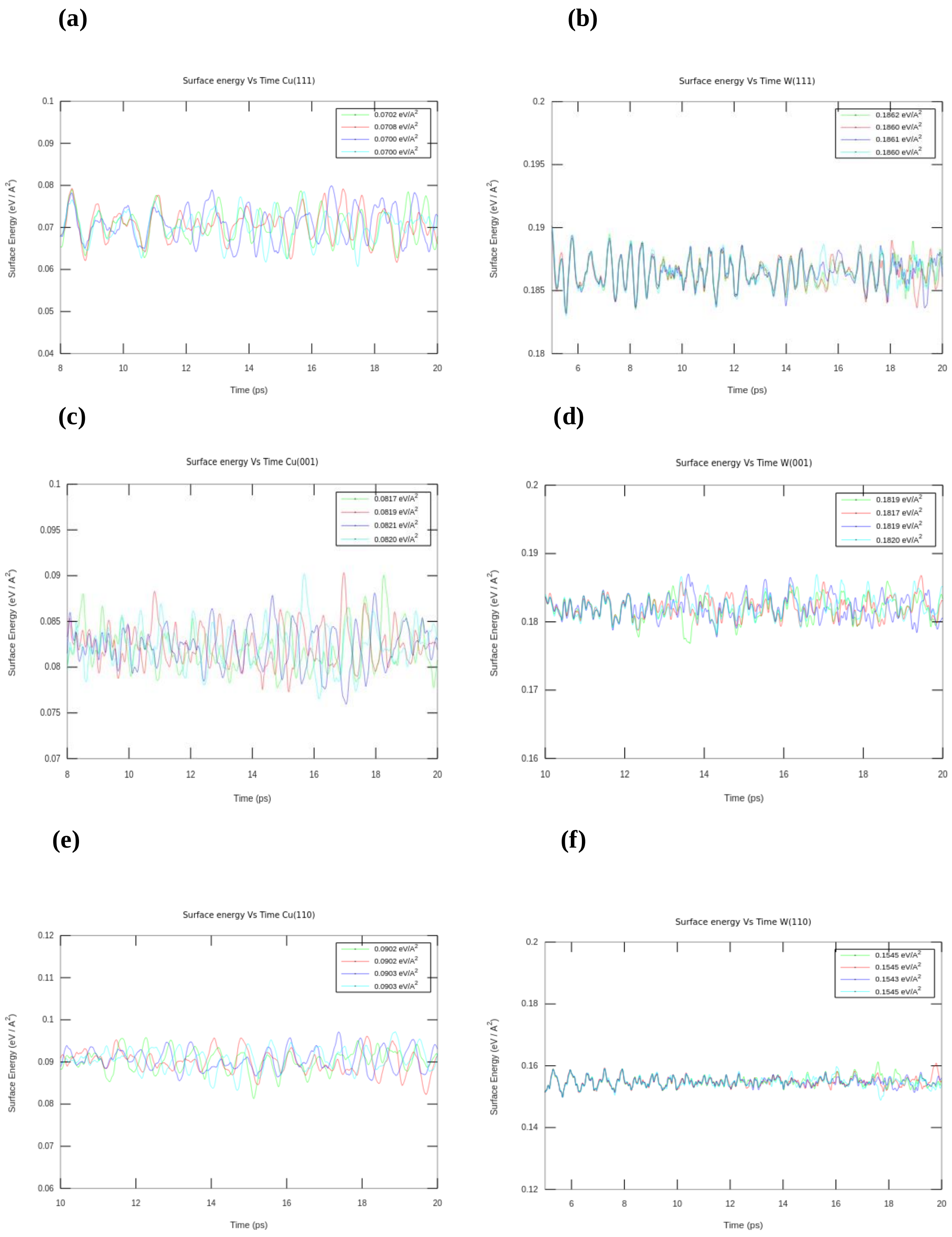

Figure 10. Surface energy of Cu and W at 350K and different seeds

Below are the results of the surface energy of Cu and W at 400k and at different seeds.

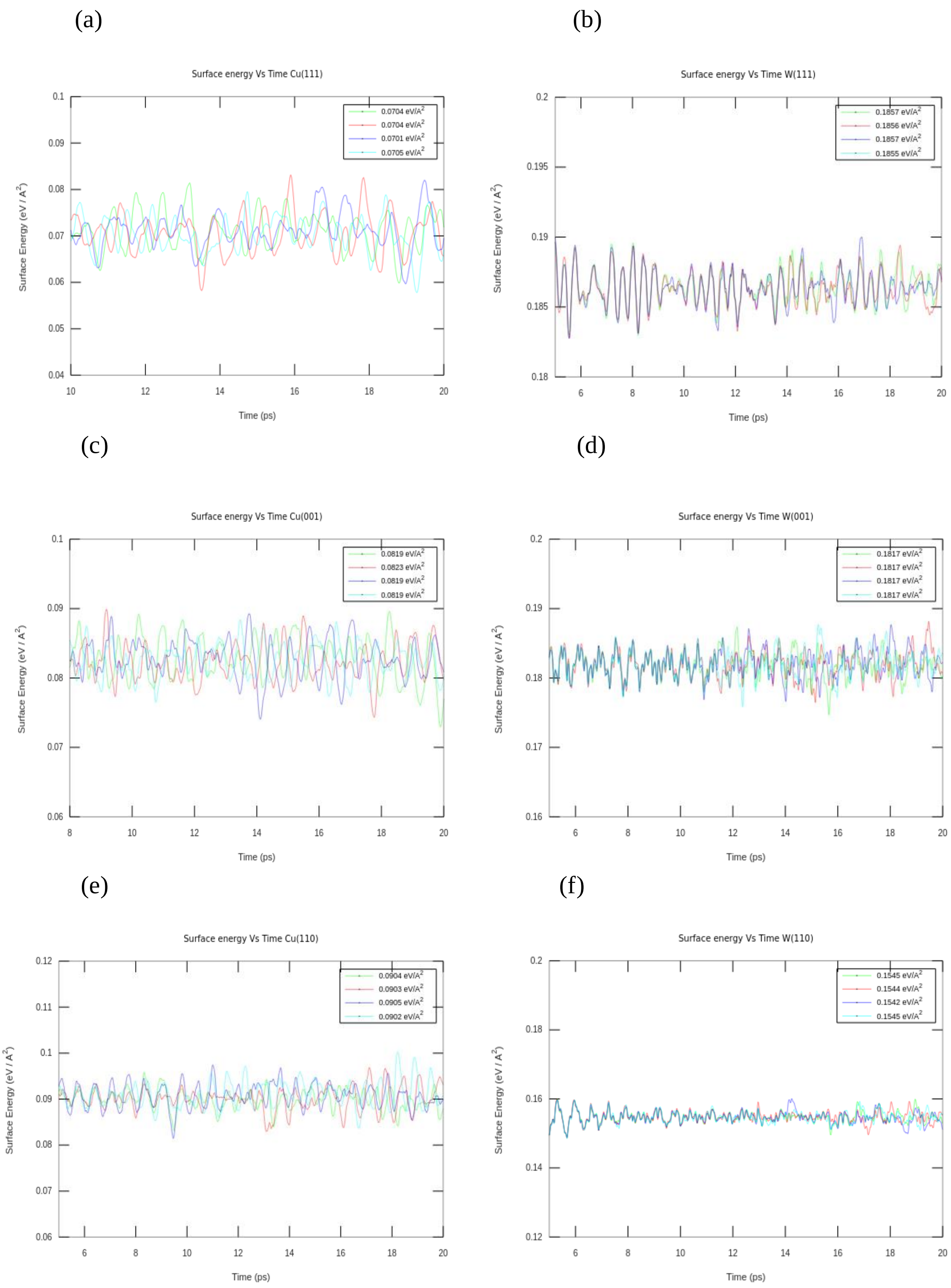

Figure 11. Surface energy of Cu and W at 400K and different seeds

Table 3a.

Surface Energy calculation of Copper (F.C.C.) and Tungsten (BCC) at 300K. Reference from [6], [9]

Metal	hkl	Surface Energy (eV/ Å²) at different seeds from MD calculations				Experiment (eV/Å²). Cu from[7]	Experiment (eV/Å²). W from[10]
		1	2	3	4		
Copper (Cu)	(111)	0.0702	0.0702	0.0701	0.0702	0.0775 [a]	
	(001)	0.0819	0.0821	0.0820	0.0821	0.0828 [a]	
	(110)	0.0904	0.0905	0.0905	0.0904	0.0889 [a]	
Tungsten (W)	(111)	0.1859	0.1859	0.1855	0.1859		0.1930 [b]
	(001)	0.1819	0.1819	0.1819	0.1818		0.1820 [b]
	(110)	0.1545	0.1547	0.1544	0.1546		0.1500 [b]

[a] Experimental, Ref.[7].

[b] Experimental, Ref.[10].

The results in Table 3a above agrees with [6] and [7, 11] [9] and also with the known trend of the surface energies of FFC and BCC across the different surface. As established In the result above for the FCC metal, the surface energy increase in the order $\gamma(111) < \gamma(001) < \gamma(110)$ and BCC in the opposite direction $\gamma(110)<\gamma(001)<\gamma(111)$. This provides the proficiency level of the embedded atom method [10], procedure and script used in this study.

This gave the go-ahead to use the script in further studies of Copper and Tungsten across various temperatures and seeds to establish consistency in surface trends and properties.

Table 3b.
Surface Energy calculation of Copper (F.C.C.) and Tungsten (BCC) at 350K.

Metal	hkl	Surface Energy (eV/ Å²) at different seeds from MD calculations			
		1	2	3	4
Copper (Cu)	(111)	0.0702	0.0708	0.0700	0.0700
	(001)	0.0817	0.0819	0.0821	0.0820

	(110)	0.0902	0.0902	0.0903	0.0903
Tungsten (W)	(111)	0.1862	0.1860	0.1861	0.1860
	(001)	0.1819	0.1817	0.1819	0.1820
	(110)	0.1545	0.1545	0.1543	0.1545

Table 3c.

Surface Energy calculation of Copper (F.C.C.) and Tungsten (BCC) at 400K.

Metal	hkl	Surface Energy (eV/ Å^2) at different seeds from MD calculations			
		1	2	3	4
Copper (Cu)	(111)	0.0704	0.0704	0.0701	0.0705
	(001)	0.0819	0.0823	0.0819	0.0819
	(110)	0.0904	0.0903	0.0905	0.0902
Tungsten (W)	(111)	0.1857	0.1856	0.1857	0.1855
	(001)	0.1817	0.1817	0.1815	0.1817
	(110)	0.1545	0.1544	0.1542	0.1545

Table 4a.

Metal	Temperature (K)	Surface Energy (eV/ Å^2) at different seeds from MD calculations (111)			
		1	2	3	4
Copper (Cu)	300	0.0702 +/- 0.0062	0.0702 +/- 0.0062	0.0701 +/- 0.0062	0.0702 +/- 0.0062
	350	0.0702 +/- 0.0067	0.0708 +/- 0.0067	0.0700 +/- 0.0067	0.0701 +/- 0.0067
	400	0.0704	0.0704	0.0701	0.0705

		+/- 0.0070	+/- 0.0070	+/- 0.0070	+/- 0.0070
Tungsten (W)	300	0.1859 +/- 0.0085	0.1859 +/- 0.0085	0.1855 +/- 0.0085	0.1859 +/- 0.0085
	350	0.1862 +/- 0.0070	0.1860 +/- 0.0070	0.1861 +/- 0.0070	0.1860 +/- 0.0070
	400	0.1857 +/- 0.0094	0.1856 +/- 0.0094	0.1857 +/- 0.0094	0.1855 +/- 0.0094

Table 4b.

Metal	Temperature (K)	Surface Energy (eV/ Å²) at different seeds from MD calculations (001)			
		1	2	3	4
Copper (Cu)	300	0.0819 +/- 0.0036	0.0821 +/- 0.0036	0.0820 +/- 0.0036	0.0821 +/- 0.0036
	350	0.0817 +/- 0.0039	0.0819 +/- 0.0039	0.0821 +/- 0.0039	0.0820 +/- 0.0039
	400	0.0819 +/- 0.0041s	0.0823 +/- 0.0041	0.0819 +/- 0.0041	0.0819 +/- 0.0041
Tungsten (W)	300	0.1819 +/- 0.0100	0.1819 +/- 0.0100	0.1819 +/- 0.0100	0.1818 +/- 0.0100
	350	0.1819 +/- 0.0081	0.1817 +/- 0.0081	0.1819 +/- 0.0081	0.1820 +/- 0.0081
	400	0.1817 +/- 0.0108	0.1817 +/- 0.0108	0.1815 +/- 0.0108	0.1817 +/- 0.0108

Table 4c.

Metal	Temperature (K)	Surface Energy (eV/ Å²) at different seeds from MD calculations (110)			
		1	2	3	4
Copper (Cu)	300	0.0904 +/- 0.0056	0.0905 +/- 0.0056	0.0905 +/- 0.0056	0.0904 +/- 0.0056
	350	0.0902 +/- 0.0059	0.0902 +/- 0.0059	0.0903 +/- 0.0059	0.0903 +/- 0.0059
	400	0.0904 +/- 0.0060	0.0903 +/- 0.0060	0.0905 +/- 0.0060	0.0902 +/- 0.0060
Tungsten (W)	300	0.1545 +/- 0.0047	0.1547 +/- 0.0047	0.1544 +/- 0.0047	0.1546 +/- 0.0047
	350	0.1545 +/- 0.0049	0.1545 +/- 0.0049	0.1543 +/- 0.0049	0.1545 +/- 0.0049
	400	0.1545 +/- 0.0052	0.1544 +/- 0.0052	0.1542 +/- 0.0052	0.1545 +/- 0.0052

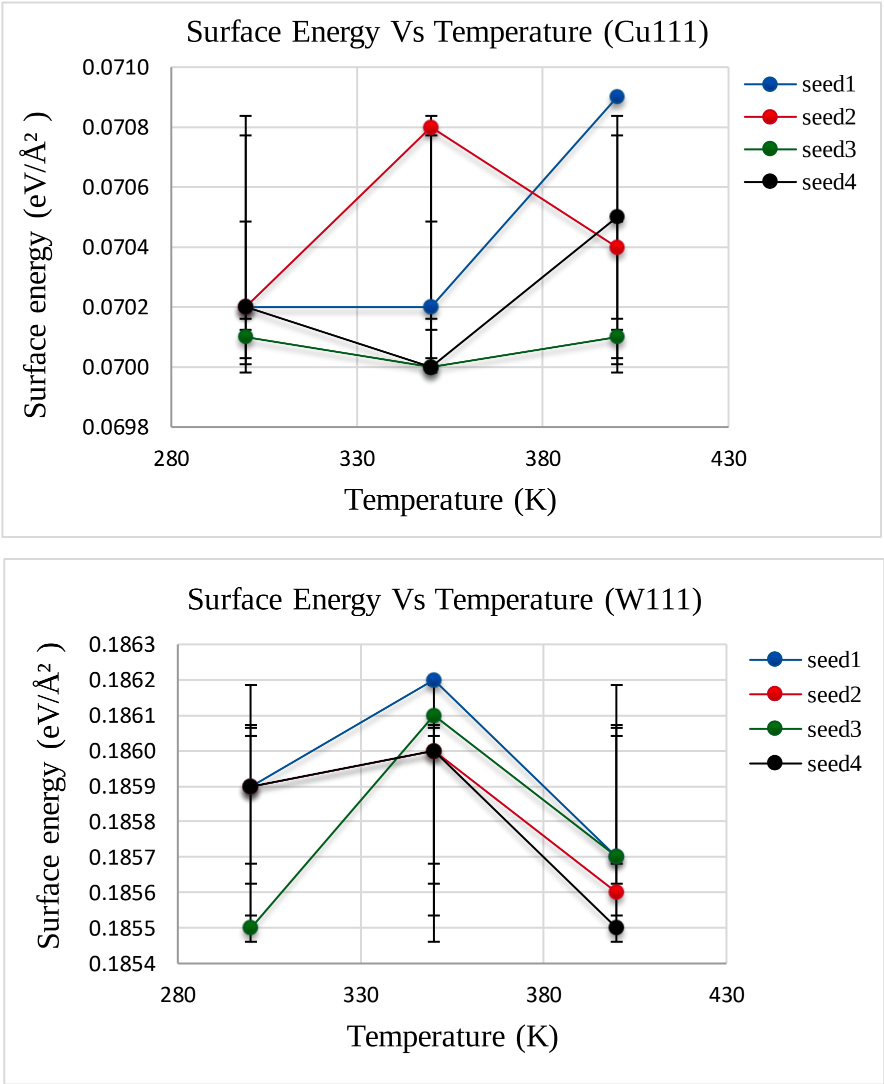

Figure 12. (111) Surface enegies of Cu and W across various Temperatures.

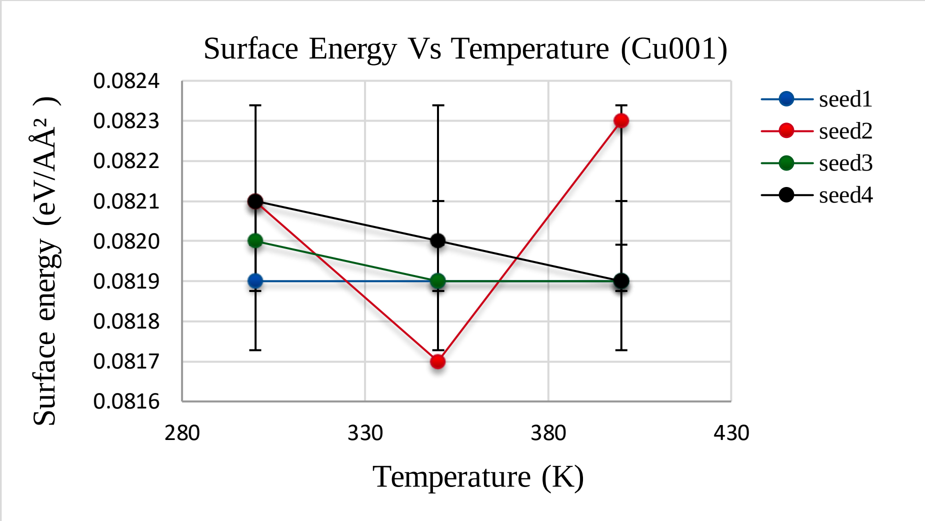

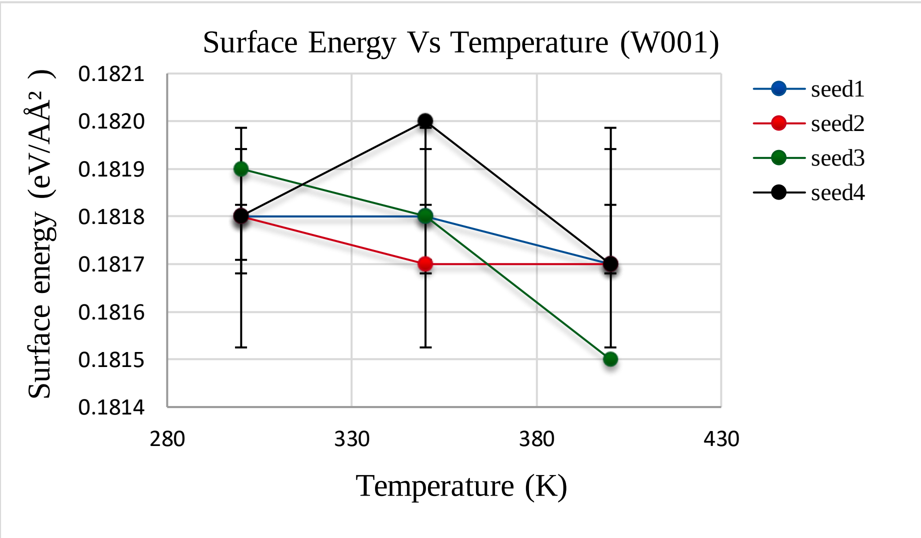

Figure 13. (001) Surface enegies of Cu and W across various Temperatures.

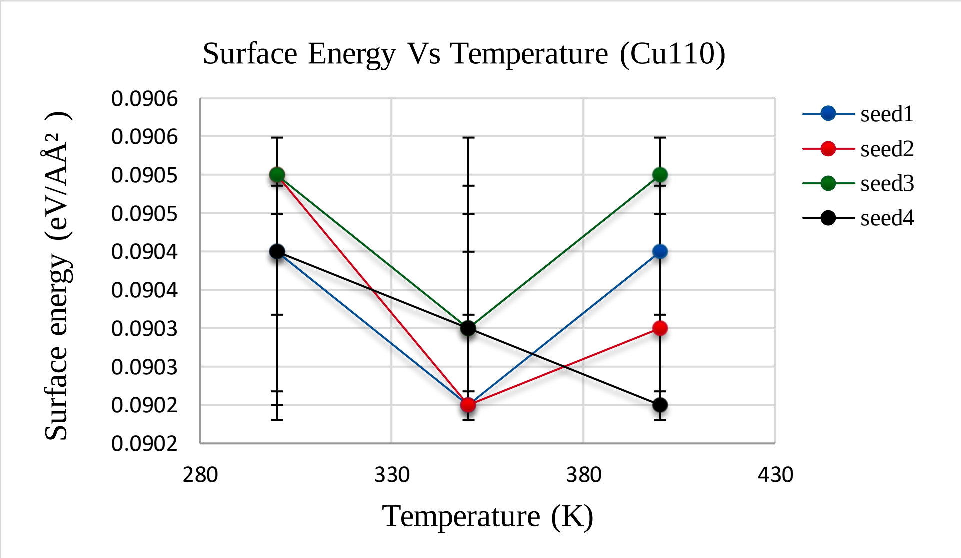

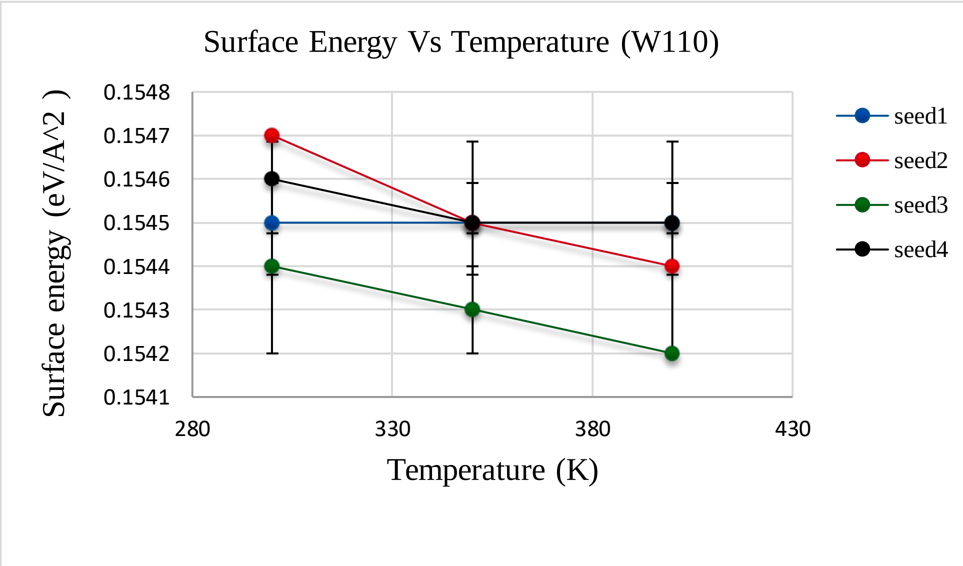

Figure 14. (110) Surface enegies of Cu and W across various Temperatures.

4.2 Comparative Study and trend analysis

The arrangement of the atom from Figure 9 - 11 above agrees with available Studies of crystallography, which reveals that crystallographic directions and orientation of atoms in different surfaces, is a significant determinant of the surface energy of a material along various surfaces. This is evident in the difference in surface energy values between elements (copper – copper and Tungsten - Tungsten) and across elements (Copper and Tungsten). As already stated above, in between the element FCC metal, FCC surface energies increase in the order of magnitude $\gamma(111) < \gamma(001) < \gamma(110)$ and while BCC in the opposite order of magnitude $\gamma(110) < \gamma(001) < \gamma(111)$, from studies this due to the anisotropic properties of FCC and BCC.

By visual observation and experimental data, it observed in the mode arrangement of atoms in various surfaces of Copper that (110) is the most loosely arranged surface followed by the (001) surface while (111) surface is the least loose arrangement there in the Copper crystallographic arrangement to earn this surface the "close-packed" title. By extension, this is also seen in Tungsten in a similar order, but this difference is in how these various arrangements affect the values of the surface energies.

Figure 9 – 11, backed up by data from table 3a – 3c, once again presents, first, the consistency and accuracy of the result obtained via running each simulation for each surface with various seed phrases across three different temperatures with the outcome of little to know changes in the value of results for same surface under same temperature and pressure in four other seed phases. The result has passed the sanity checklist, as the value difference after each run is less than 10%.

In principle, surface energy depends on the net inward cohesive force, and so surface energy decreases with increasing temperature. The results in Table 4a – 4c and Figure 11 – 13 show inconsistency in trend regarding this attribute across both Copper and Tungsten. In most cases, the surface energies are observed dropping in insignificant amounts as expected, in other instances remaining the same as in the case of W(111) at 300K upon running the simulation several times. To get this, it was realised that accuracy in the consistency of atomic simulation of metal properties is inherently dependent on the nature of the nuclear potential used for each element and simulation. These potentials are just an approximate of the attribute of each metal and not the exact thing. Hence various potential tests produce different types of trends as regards temperature and surface energy value.

Nevertheless, upon a head-to-head comparison of Copper and Tungsten, results reveal that all copper surfaces have significantly lower energies than the reciprocal surface in Tungsten. For example, the (001) surface of Copper has considerably more atoms at its surface and the same surface in Tungsten (Fig. 7a and 7f), hence many of the atoms at this surface for Copper are already used for bond formation will translate to lower excess energy available for other use. This will be the opposite for Tungsten (001) surface. This trend continues in all surfaces. These trends uncovered that the first copper close-pack surface (111) had lower surface energy than all other surfaces. The (110) surface appears to be the most reactive surface with the highest surface energy value, the direct opposite for Tungsten. This trend is seen reoccurring almost in the same manner across different temperatures and seeds, as indicated in Table 3a - c. Another observation across the element is copper surface head-to-head with Tungsten considerably has lower surface energy than Tungsten in all directions.

SUMMARY AND FUTURE DIRECTION

This paper achieved the following objectives; firstly, it gave a comprehensive approach to how surface energy for metal or material can be calculated from Molecular dynamic simulation via lammps and Ovito through the embedded atom method. Second, it sufficiently presents the values of the surface energy of Tungsten.

In conclusion, the data collected in this thesis supports the use of Copper as a preferred option for high electric field systems due to its lower surface energies compared to Tungsten across three important material surfaces analysed. However, this advantage is only temporary before vacuum arc damage occurs, which is a well-known issue. Despite previous studies in [11] showing the possibility of Tungsten surface modification through the formation of nanotips in specific crystallographic directions using femtosecond laser irradiation and exposure to a strong DC electric field, the careful examination of Tungsten surface energy in this thesis suggests that Tungsten has the potential to be a viable option for the future due to its higher but stable surface energies across all surfaces considered.

These findings indicate that Tungsten may last longer than Copper. However, further research is required to explore ways to maintain the stability of Tungsten's atomic structure and lower its surface energy to make it a better option than Copper. Therefore, this research is not yet conclusive. Future studies should focus on simulating and comparing the performance of Copper and Tungsten using advanced tools such as the Finite Element Method (FEM). To use this tool, additional parameters such as surface elastic constants (C_{11}, C_{12}, C_{44}), shear modulus, and bulk modulus, which are beyond the scope of this work, must be considered.

REFERENCES

[1] A. Grudiev, S. Calatroni, and W. Wuensch, "Erratum: New local field quantity describing the high gradient limit of accelerating structures [Phys. Rev. ST Accel. Beams 12, 102001 (2009)]," *Phys. Rev. ST Accel. Beams*, vol. 14, no. 9, p. 99902, Sep. 2011, doi: 10.1103/PhysRevSTAB.14.099902.

[2] Z. Insepov, J. Norem, and S. Veitzer, "Atomistic self-sputtering mechanisms of rf breakdown in high-gradient linacs," *Nucl. Instruments Methods Phys. Res. Sect. B Beam Interact. with Mater. Atoms*, vol. 268, no. 6, pp. 642–650, 2010, doi: 10.1016/j.nimb.2009.12.016.

[3] Z. Insepov, J. Norem, T. Proslier, D. Huang, S. Mahalingam, and S. Veitzer, "Modeling rf breakdown arcs," 2010, [Online]. Available: http://arxiv.org/abs/1003.1736.

[4] A. Descoeudres, T. Ramsvik, S. Calatroni, M. Taborelli, and W. Wuensch, "dc breakdown conditioning and breakdown rate of metals and metallic alloys under ultrahigh vacuum," *Phys. Rev. ST Accel. Beams*, vol. 12, no. 3, p. 32001, Mar. 2009, doi: 10.1103/PhysRevSTAB.12.032001.

[5] K. Nordlund and F. Djurabekova, "Defect model for the dependence of breakdown rate on external electric fields," *Phys. Rev. ST Accel. Beams*, vol. 15, no. 7, p. 71002, Jul. 2012, doi: 10.1103/PhysRevSTAB.15.071002.

[6] V. B. Shenoy, "Atomistic calculations of elastic properties of metallic fcc crystal surfaces," *Phys. Rev. B - Condens. Matter Mater. Phys.*, vol. 71, no. 9, pp. 1–11, 2005, doi: 10.1103/PhysRevB.71.094104.

[7] Y. Mishin, M. J. Mehl, D. A. Papaconstantopoulos, A. F. Voter, and J. D. Kress, "Structural stability and lattice defects in copper: Ab initio, tight-binding, and embedded-atom calculations," *Phys. Rev. B - Condens. Matter Mater. Phys.*, vol. 63, no. 22, pp. 2241061–22410616, 2001, doi: 10.1103/PhysRevB.63.224106.

[8] P. L. Williams, Y. Mishin, and J. C. Hamilton, "An embedded-atom potential for the Cu-Ag system," *model. Simul. Mater. Sci. Eng.*, vol. 14, no. 5, pp. 817–833, 2006, doi: 10.1088/0965-0393/14/5/002.

[9] D. R. Mason, D. Nguyen-Manh, and C. S. Becquart, "An empirical potential for simulating vacancy clusters in tungsten," *J. Phys. Condens. Matter*, vol. 29, no. 50, 2017, doi: 10.1088/1361-648X/aa9776.

[10] J. M. Zhang, F. Ma, and K. W. Xu, "Calculation of the surface energy of fee metals with modified embedded-atom method," *Chinese Phys.*, vol. 13, no. 7, pp. 1082–1090, 2004, doi: 10.1088/1009-1963/13/7/020.

[11] H. Yanagisawa *et al.*, "Laser-induced asymmetric faceting and growth of a nano-protrusion on a tungsten tip," *APL Photonics*, vol. 1, no. 9, 2016, doi: 10.1063/1.4967494.

Appendix

I. Simulation script

```
# Find surface energy fcc and bcc
# Get Total Energy of the surface model and other parameters
# Joseph Theophilus Odubena, 2022

# ---------- Initialize Simulation ---------------------
clear
units metal
dimension 3
boundary p p p
atom_style atomic
atom_modify map array

# ---------- Create Atoms ---------------------
lattice         fcc 3.615

region          closebox block 0 25 0 25 0 25 units box
region          upside block   0 25 0 25 25 45 units box
region          downside block  0 25 0 25 -25 0 units box

region          simulationdomain union 3 upside downside closebox

create_box      1 simulationdomain

lattice fcc     3.615 orient x 1 0 0 orient y 0 1 0 orient z 0 0 1
create_atoms    1 region closebox

# ---------- Define Interatomic Potential ---------------------
pair_style      eam/alloy
pair_coeff      * * Cu01.eam.alloy.Mishin.txt Cu

mass 1 63.546

# ---------- Define Settings ---------------------
compute pot_energy all pe
compute p_energy all ke
compute myTemp all temp

variable tp equal "step"
variable kin_e equal "ke"
variable pot_e equal "pe"
variable temperature equal "temp"
variable natoms equal "count(all)"            # count all atoms
variable L_x equal "lx"
variable L_y equal "ly"

# -------------------EQUILIBRATION-------------------

timestep 0.001
thermo 100

velocity all create 300.0 12345
reset_timestep 0

# relax system at 300 K

fix relax_system all npt temp 300 300 0.1 iso 0.0 0.0 1.0

# =================== define data export ================

shell mkdir dump-open-relaxation
dump 1 all custom 100 ./dump-open-relaxation/dump* id x y z
fix      6 all print 1  " ${tp} ${kin_e} ${pot_e} ${temperature}
${L_x} ${L_y} ${natoms} " file open-relaxation-energy.txt screen no

#==================== run relaxation ========================
run     20000
unfix   relax_system
```

```
# Find surface energy fcc and bcc
# Get bulk Energy and other parameters
# Joseph Theophilus Odubena, 2022

# ---------- Initialize Simulation ---------------------
clear
units metal
dimension 3
boundary p p p
atom_style atomic
atom_modify map array

# ---------- Create Atoms ---------------------
lattice         fcc 3.615
region          closebox block 0 25 0 25 0 25 units box
create_box      1 closebox
lattice         fcc 3.615 orient x 1 0 0 orient y 0 1 0 orient z 0 0 1
create_atoms    1 region closebox

# ---------- Define Interatomic Potential ---------------------
pair_style      eam/alloy
pair_coeff      * * Cu01.eam.alloy.Mishin.txt Cu

mass 1 63.546

# ---------- Define Settings ---------------------
compute pot_energy all pe
compute p_energy all ke
compute myTemp all temp

variable tp equal "step"
variable kin_e equal "ke"
variable pot_e equal "pe"
variable temperature equal "temp"
variable natoms equal "count(all)"            # count all atoms
variable L_x equal "lx"
variable L_y equal "ly"

# -------------------EQUILIBRATION-------------------#

timestep 0.001
thermo 100

velocity all create 300.0 12345
reset_timestep 0

# relax system at 300 K
fix relax_system all npt temp 300 300 0.1 iso 0.0 0.0 1.0

# =================== define data export ================

shell mkdir dump-periodic-relaxation
dump 1 all custom 100 ./dump-periodic-relaxation/dump* id x y z
fix      6 all print 1  " ${tp} ${kin_e} ${pot_e} ${temperature}
${L_x} ${L_y} ${natoms}" file periodic-relaxation-energy.txt screen no

#==================== run relaxation ========================
run     20000
unfix   relax_system


print "All done"
```

NON-EXCLUSIVE LICENCE TO REPRODUCE THESIS AND MAKE THESIS PUBLIC